EJFA Emirates Journal of Food and Agriculture

Emirates Journal of Food and Agriculture 36: 1–10
doi: 10.3897/ejfa.2024.123913

RESEARCH PAPER

Metabolite profiling of sugar and phenolics provide clues for postharvest anthocyanin accumulation in detached leaves of lemon balm for possible utilization in food products

Pritam Kumar Dey[1], Manisha Lakhanpal[2], Adinpunya Mitra[1]

1 *Natural Product Biotechnology Group, Agricultural and Food Engineering Department, Indian Institute of Technology Kharagpur, Kharagpur – 721 302, West Bengal, India*

2 *Department of Forest Products, Dr YS Parmar University of Horticulture and Forestry, Nauni, Solan – 173 230, Himachal Pradesh, India*

Corresponding author: Adinpunya Mitra (adin@iitkgp.ac.in)

Academic editor: Luca Rastrelli ♦ **Received** 25 March 2024 ♦ **Accepted** 10 May 2024 ♦ **Published** 27 May 2024

Abstract

Melissa officinalis L., an aromatic herb is commonly known as lemon balm for its lemon fragrance. This study reports the outcome of simulation experiment conducted inside the plant growth chamber followed by conducting the same experiment in realtime condition in open environment for 21 days to see the response of postharvest lemon balm leaves in accumulating anthocyanin pigments. Detached leaves were found to accumulate anthocyanin up to 21 days in both the cases. Simulation experiment showed cyanidin concentration of 2.36 ± 0.37 g Kg^{-1} whereas it was 1.78 ± 0.49 g Kg^{-1} in realtime experiment. The accumulated anthocyanin appeared stable in different buffer solutions with variable pH ranges. Further, degradation of the major internal pool of volatile was observed in both the cases. However, rosmarinic acid content was found to be increased in realtime experiment in comparison to simulation experiment which was just unlike of cyanidin. Several primary metabolites mostly sugars were found to be varied between the detached leaves generated from the two experiments. Sucrose was found to be the highest contributors among all the primary metabolites detected in red leaves from simulation experiment whereas it is talose in the case of realtime experiment. Various food products were also prepared from these value-added leaves to demonstrate its immediate application potential.

Keywords

Lemon balm, simulation, anthocyanin, postharvest treatment, value-addition

Introduction

Medicinal and aromatic plants both are now widely used in food products alongside their regular utility in cosmetics and herbal medicinal products (Taban et al. 2021). In order to follow the instruction of WHO, food industries are always looking for low-processed food products derived from medicinal plants to replace their synthetic counterpart available in the market (Burt 2004). In this circumstances, value-added products made by minor postharvest processing from medicinal herbs could be the ideal candidates for such purpose (Rao et al. 2022). Lemon balm (*Melissa officinalis* L.), is an aromatic herb from the family Lamiaceae commonly known for its lemon fragrance, grows well in temperate and subtropical regions. Fresh as well as dried aerial parts of this plant is also widely used in traditional medicine and herbal tea preparation (Meftahizade et al. 2010). In this context, lemon balm leaves hold a great promise to generate postharvest value-added products such as anthocyanin pigments as reported in a recent literature (Dey et al. 2023).

Copyright *Dey PK, et al.* This is an open access article distributed under the terms of the Creative Commons Attribution License (CC-BY 4.0), which permits unrestricted use, distribution, and reproduction in any medium, provided the original author and source are credited.

As the lead obtained in the above instance was carried out under a temperature-controlled glasshouse condition, there is a need to demonstrate this technology in open environment. The under-utilized hilly terrains of Indian Himalayan region, particularly Himachal Pradesh would be an ideal choice for conducting such outdoor experiments as *M. officinalis* plants are befittingly acclimatized and cultivated there. Adoption of this technology by the rural people of Himachal Pradesh state could also improve their livelihood opportunities and pave a way for creating new cottage industries both for local consumption and commercial export to food industries. The outcome if successful, could vouch for the simple home-scale adoption of this technology by the people those regions for possible application in food products such as lemon balm herbal tea, topping of cakes with natural colouration.

Before carrying out field level trials in an open environment, we decided to conduct the experiment in a plant growth chamber by mimicking the fluctuating air temperatures that prevail during the summer months at low altitudes of Himachal Pradesh. Subsequently, Nauni, (altitude 1500 m), was chosen as the place to conduct experiment in the open environment.

Although Dey et al. (2023) made a targeted approach for generating postharvest anthocyanin in lemon balm leaves upon continuous incubation in water, the science behind this unusual anthocyanin accumulation remained elusive. This manuscript reports comparative accumulation of postharvest anthocyanin in lemon balm leaves upon continuous incubation in water which was carried out at two pre-defined conditions. The status of volatile and non-volatile metabolites and rosmarinic acid in postharvest *M. officinalis* leaves were also measured. Further, we compared the status of soluble sugars through semi-targeted profiling. As sugars are the main source of any metabolism including accumulation of phenolics, we anticipated that undertaking a study on metabolite profiling of sugars from postharvest leaves could shed light on the possible biochemical pathways associated with *de novo* accumulation of anthocyanin in detached lemon balm leaves. Finally, we also report preparations of a few food products from these value-added leaves which can easily be taken up for regular household consumption purpose such as ice cubes enriched with value-added lemon juice, herbal tea and topping of cakes Attempts were also made to garnish fruit salad by value-added lemon-juice after mixing it with the fresh cream.

Methods

Plant material and experimental set up

Postharvest incubation experiments with detached leaves were done in vials according to the published method of Dey et al. (2023). For simulation experiment, these vials were incubated for 21 days inside the plant growth chamber (LabTech India Pvt Ltd.) at Natural Product Biotechnology Group (Agricultural and Food Engineering Department, Indian Institute of Technology Kharagpur, Kharagpur, West Bengal, India), having a temperature cycle starting from 24 °C and going down to 4 °C (with a decreasing rate of 4 °C/2.5 h) and then again increasing to 20 °C (with an increasing rate of 4 °C/2.5 h), using warm fluorescent LED light (9500 ± 500 lux) under a 12 h photoperiod. Similarly, realtime experiment was conducted for 21 days in the open environment of Dr YS Parmar University of Horticulture and Forestry (Nauni, Solan, Himachal Pradesh, India) keeping the light intensity same as simulation (~ 10000 lux) during autumn (~ 12 h photoperiod).

pH stability test and quality characterization

Extraction of anthocyanin was done from 50 mg dry leaves using liquid N_2 in 2 mL of pure methanol: 1 N HCl (85:15). After vortexing, these extracts were then sonicated for 30 min followed by centrifugation for 15 min at 7000 g. Supernatant were then collected and used to check the effect of different pH (ranging from pH 1.0 to pH 11.0) on the stability of anthocyanin using a spectrophotometer (Shimadzu UV 1800, Japan) in single scan mode. Buffers used in this experiment were prepared as stated by Qin et al. (2010). Extracts (100 µL) were added to 900 µL of buffers and UV-Vis spectra were recorded. Colour density (CD), colour intensity (CI) and browning index (BI) of the anthocyanin were also measured according to Cisse et al. (2011) in each of these buffer systems.

HPLC quantification of cyanidin

Total anthocyanin was pulled twice from 50 mg of dried leaf sample resulted in 2 mL of extract which then concentrated to 0.25 mL under the flow of nitrogen before analysed in HPLC. HPLC analysis for anthocyanin followed by acid hydrolysis of extracted anthocyanin and subsequent analysis of anthocyanidin was done following a previously published work Dey et al. (2023) with slight modification in elution gradient. The mobile phase consisted of A (0.4% TFA in water) and B (0.4% TFA in acetonitrile). The protocol for elution was 0–2 min 10% B, 2–5 min 15% B, 5–10 min hold 15% B, 10–15 min 22% B, 15–45 min 65% B, 45–50 min 90% B with a flow rate of 1 mL min^{-1} and injection volume was 50 µL. Quantification of cyanidin was done by comparing the retention time and absorption spectrum of the samples with that of authentic standard.

HPLC quantification of rosmarinic acid

Extraction was done in 1 mL of 80% methanol from the 20 mg dried leaf samples. This was successively followed by vortexing and sonication up to 30 min. Finally, the centrifugation of the extract was done at 10,000 rpm for 15 min. Identification and quantification of rosmarinic

acid in HPLC was done following the published method of Dey et al. (2023) with slight modification in elution gradient. The mobile phase consisted of A (0.1% TFA in water) and B (acetonitrile). The protocol for elution was 0–2 min 10% B, 2–5 min 15% B, 5–10 min hold 15% B, 10–15 min 22% B, 15–45 min 65% B, 45–50 min 90% B with a flow rate of 1 mL min^{-1} and injection volume was 50 µL.

GC-MS quantification of internal pool of volatile compounds

Extraction and quantification of internal pool of volatile compounds was carried out from 50 mg of dried leaves as described by Bimolata et al. (2023). Firstly, internal pool of volatiles was extracted from the dried leaves in 1 mL of hexane with the help of liquid N_2. Then, the supernatant was collected after centrifugation and treated with anhydrous sodium sulphate. After removal of sodium sulphate again by centrifugation extract was purged to 50 µL using nitrogen gas. Then 1 µL of ethyl hexanoate prepared in hexane (1:1000 v/v) was added to it as an internal standard. Finally, 1 µL sample was injected in the GC-MS (Trace™ 1300 equipped with ISQ QD single quadrupole mass spectrometer, Thermo Fisher Scientific) and autosampler AI1310. Column used for the separation was TG-5MS (30 m × 0.25 mm, 0.25 µm, Thermo Fisher Scientific). Split ratio for the injection was 1:10. The inlet temperature was maintained at 260 °C throughout the time. Oven temperature was initially set at 50 °C for 2 min then increased at a rate of 2 °C/min to 60 °C and held for 2 min. This was followed by an increase to 210 °C at a rate 3 °C/min and again held for 2 min. Finally, the temperature was held for 7 min upon reaching 270 °C at 10 °C/min rate. Flow rate of the Helium (carrier gas) was maintained at 1 mL/min. MS transfer line temperature and MS ion source temperature were kept at 280 °C and 200 °C respectively. Electron impact was set at 70 eV with a scanning range of 40–600 amu. NIST 20 library was used to identify the compounds after comparing with the mass spectra to that of database (National Institute of Standards and Technology, Gaithersburg, USA) linked with Xcalibur 3.0.63 software (Thermo Scientific). Ethyl hexanoate was used as internal standard for quantification of these volatile compounds and expressed in nano mole per kilogram of dry weight of sample. Retention index of those compounds was also calculated in relative to the standard solution of n-alkanes (C8–C20, Sigma-Aldrich, USA).

Extraction and qualitative analysis of primary metabolites

Primary metabolites were analyzed in GC-MS, following a modified method of Kotamreddy et al. (2020). Dried leaf (10 mg) was first extracted in 1 mL of 100% HPLC grade methanol with the addition of 20 µL each of BHT and norleucine as internal standards (0.2 mg ml^{-1} concentration) followed by incubation at 70 °C for 15 min. After that, supernatant was vacuum dried followed by addition of methoxyamine-HCl for 120 min at 37 °C. Finally, it was derivatization with BSTFA at 70 °C for 1 h. Then, 1 µL of derivatized metabolites were injected with a split ratio of 30:1 in GC–MS (TRACE™ 1300, Thermo Scientific) for analysis. TG-5MS column was used for the separation with helium as a carrier gas with flow rate of 1 ml min^{-1}. The inlet temperature of injector was kept at 280 °C. Initial column oven temperature was held 70 °C for 4 min, and then increased to 300 °C at a rate of 5 °C min^{-1} and held for 10 min. Ionization mode of single quadrupole mass spectrometer was set at 70 eV with a scanning range of m/z 40–600 atomic mass unit. NIST 20 mass spectral library was used for identification of compounds. The relative abundance of various metabolites was calculated as the ratio of peak area of an individual compound to that of the total area. Retention index of those compounds was also calculated in relative to the standard solution of n-alkanes (C10–C40, Sigma-Aldrich, USA).

Statistical analysis

The mean and standard deviation values were computed in Microsoft Excel 2019 using data from three independent biological replicates. Statistical significance of difference was analysed by Student's t test using Past 4.01 software ($p < 0.05$).

Results

Detached leaves showed a clear colour change from green to red after 21 days of incubation both in growth chamber under simulated condition and also realtime experiment in open environment which was in concurrence with the previous findings of Dey et al. (2023). This result clearly indicated that detached leaves will be not only able to survive the changing temperature in open environment but also can accumulate anthocyanin in changing temperature of high-altitude areas as evident from the simulation experiment. Further, detached leaves did not show any sign of senescence under such fluctuations of air temperature in both the cases. (Fig. 1a, b). UV-vis absorption spectra often indicate the anthocyanin colours, which is based on the λ_{max} values. However, when pH increases or decreases UV-vis absorption pattern also changes accordingly. But in case of simulation experiment, the anthocyanins are very much stable as the λ_{max} retained at 520 nm in all the pH tested except in pH 11 (Fig. 1c). Whereas, the realtime experiment showed the λ_{max} failed to retain at 520 nm in pH 9 and pH 11 (Fig. 1d). This result appears quite interesting as the anthocyanin from the detached leaves was found to be very much stable against most of the pH buffer solutions which is very unusual in general. However, this holds an enormous potential in food industry where they can be mixed with various other food items

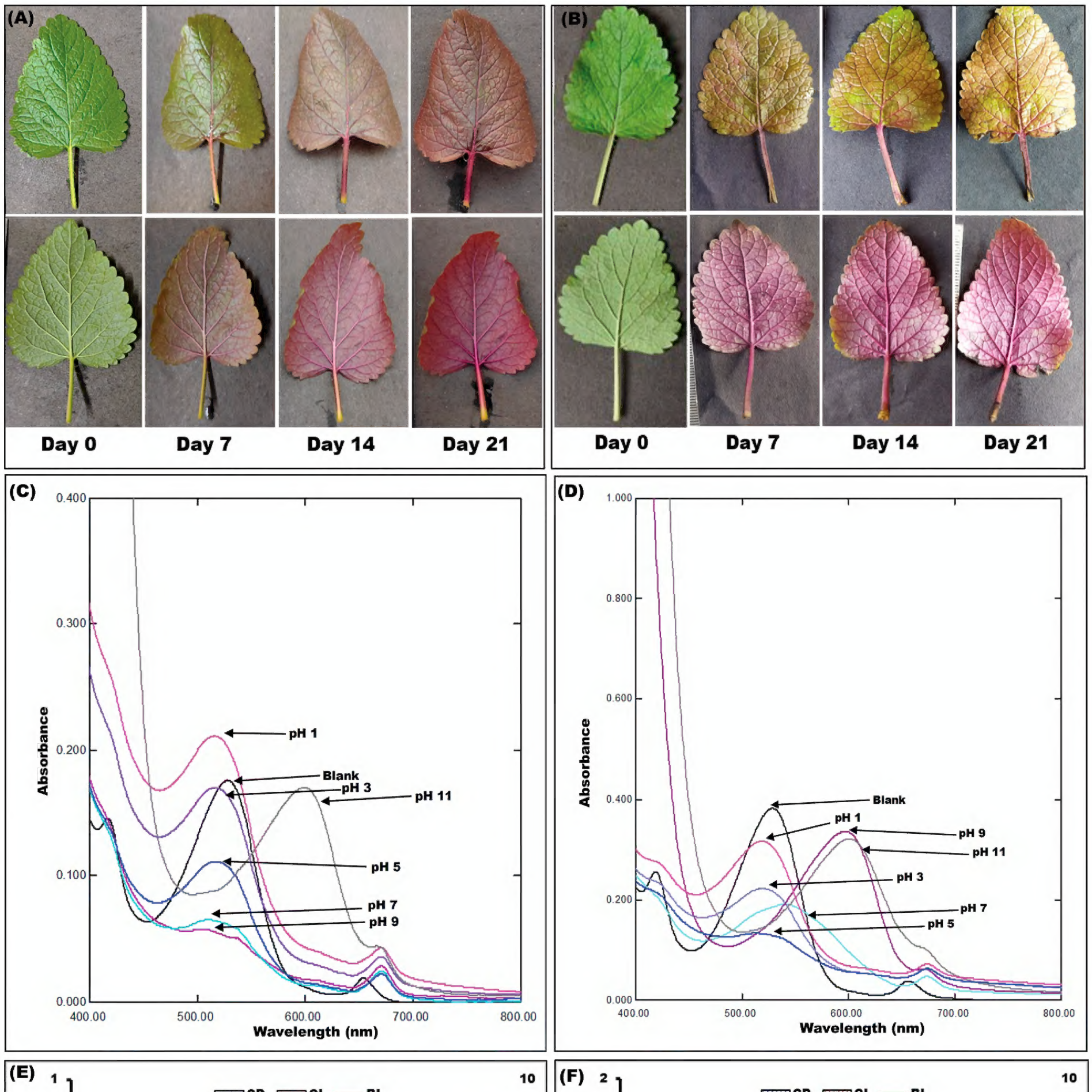

Figure 1. Formation of red colour in detached leaves of *M. officinalis* during simulation experiment in plant growth chamber (**a**) and realtime experiment in open environment (**b**). UV-vis scan plot of extracted anthocyanins under various buffer treatments for simulation experiment (**c**) and for realtime experiment (**d**). Colour density (CD), colour intensity (CI) and browning index (BI) of the extracted anthocyanin under various buffer treatments for simulation experiment (**e**) and for realtime experiment (**f**).

without losing its colour. Quality characterization result of the extracted anthocyanin both from the simulation and realtime experiment showed the same result that colour intensity was high at lower pH whereas low in higher pH. Colour density was also shown the same pattern except at pH 11 which exhibited the highest value. Browning index of the extracted anthocyanin showed the same pattern as observed with colour density (Fig. 1e, f).

A total of six different peaks were found in the HPLC generated chromatogram from the anthocyanin extract in both the cases. However, upon acid hydrolysis all reduced to just one peak which was later identified as cyanidin. The content of cyanidin in acid hydrolysed sample was higher in simulation experiment than that of real-time (Table 1). Higher cyanidin content in the simulation experiment is obvious as the experimentation was done in a growth chamber under controlled conditions. Similar HPLC based quantification done from strawberry, black currant, bilberry and red wine after acid hydrolysis showed less content in comparison with our study (Nyman and Kumpulaine 2001). HPLC analysis also showed the presence of rosmarinic acid in both the cases as a sharp peak in the chromatogram. However, rosmarinic content was found to be lower in red leaves from the simulation experiment in comparison to the content found in red leaves from the realtime experiment (Table 1), exactly opposite to the cyanidin content. This increased content of rosmarinic acid may be due to higher level of environmental fluctuations faced by the detached leaves in open environment in compare to the simulation experiment. found to be very high as compared to heat-stress mediated enhanced accumulation of rosmarinic acid reported by Pistelli et al. (2019).

Table 1. HPLC analysis of cyanidin and rosmarinic acid.

Compound Name	Content (g Kg^{-1})	
	Simulation	Realtime
Cyanidin	2.36 ± 0.37*	1.78 ± 0.49
Rosmarinic acid	21.57 ± 3.38	30.37 ± 2.83*

Data represents means ± SD of three replicates; statistically significant differences are marked by an '*' (t-test, $p < 0.05$).

GC-MS analysis revealed that in comparison to simulation experiment exo-isocitral, methyl citronellate and citronellal was found to be absent in the red leaves from realtime experiment, while a significant declination in content of α-citral, ß-citral and caryophyllene was also noticed in realtime experiment (Table 2).

A total of 26 primary metabolites detected upon analysis from both the samples (Table 3) which were mostly dominated by eighteen sugars (pentose, hexose & polysaccharides), six sugar alcohols, one phenolics and followed by one of each from sugar ketone and anhydrous sugar (Fig. 2a).

Among these, glucose (12.40%) and β-gentiobiose (7.38%) were found to be present only in the simulation experiment whereas talose (21.72%) was found to be present only in realtime experiment. Apart from that, xylofuranose, mannitol, xylitol, galactitol, gluconolactone and caffeic acid are found to be absent in simulation experiment whereas ribose, altrose and tagatofuranose are found to be absent in realtime experiment. Sucrose is the main sugar which was found to be vary most among these two experiments (32.70% in case of simulation and 5.22% in case of realtime) followed by other metabolites viz., fructose, galactose, glucose, allose, myo-Inositol, galactinol and rosmarinic acid as evident from the heatmap (Fig. 2b, c).

Table 2. Internal pool of volatiles compounds detected through GC-MS.

Compound Name	RI (Experimental)	Concentration (nmol Kg^{-1})	
		Simulation	Realtime
exo-Isocitral	1115	2738.57 ± 630.70	-
Citronellal	1126	223608.33 ± 65351.25	-
β-Citral	1169	90761.81 ± 10677.00*	39827.90 ± 9689.67
Methyl citronellate	1232	5668.83 ± 1579.75	-
α-Citral	1183	431513.27 ± 76383.39*	104261.92 ± 9490.73
Caryophyllene	1402	19615.47 ± 3407.21*	12020.56 ± 2929.59

Data represents means ± SD of three replicates; '-' indicates not detected, RI stands for Retention index, statistically significant differences are marked by an '*' (t-test, $p < 0.05$).

Table 3. Primary met abolites detected through GC-MS.

Compound Name	RI	Relative abundance (Area %)	
		Simulation	Realtime
Levoglucosan	1679	-	0.05 ± 0.01
Arabinose	1634	0.09 ± 0.01	0.27 ± 0.13
Ribose	1640	0.07 ± 0.04	-
Xylofuranose	1773	-	0.14 ± 0.03
α-Glucopyranoside	1493	0.08 ± 0.03	0.04 ± 0.01
Altrose	2077	0.24 ± 0.07	-
Fructopyranose	1854	10.38 ± 2.04	17.76 ± 0.85*
Galactose	1879	4.91 ± 0.91	4.76 ± 0.82
Glucose	1890	12.40 ± 2.50*	0.31 ± 0.19
Allose	1910	4.83 ± 1.26	9.79 ± 0.72*
Talose	1892	-	21.72 ± 0.48
Fructose	1869	10.62 ± 1.84	17.31 ± 0.51*
Tagatofuranose	1710	0.14 ± 0.04	-
Fructofuranose	1770	0.21 ± 0.05	0.72 ± 0.39*
Sucrose	2744	32.70 ± 6.62*	5.22 ± 0.66
Maltose	2237	0.40 ± 0.08	2.45 ± 0.91*
Cellobiose	3224	-	3.02 ± 0.20
β-Gentiobiose	2279	7.35 ± 1.22	-
Myo-Inositol	2075	8.03 ± 2.10	10.51 ± 0.80
Galactinol	3349	7.51 ± 0.70*	4.98 ± 0.25
Mannitol	1853	-	0.27 ± 0.02
Erythritol	1536	0.06 ± 0.01	0.07 ± 0.02
Xylitol	1705	-	0.26 ± 0.08
Galactitol	2403	-	0.14 ± 0.06
Gluconolactone	1810	-	0.08 ± 0.03
Caffeic acid	2090	-	0.12 ± 0.03

Data represents means ± SD of three replicates; '-' indicates not detected, RI stands for Retention index, statistically significant differences are marked by an '*' (t-test, $p < 0.05$).

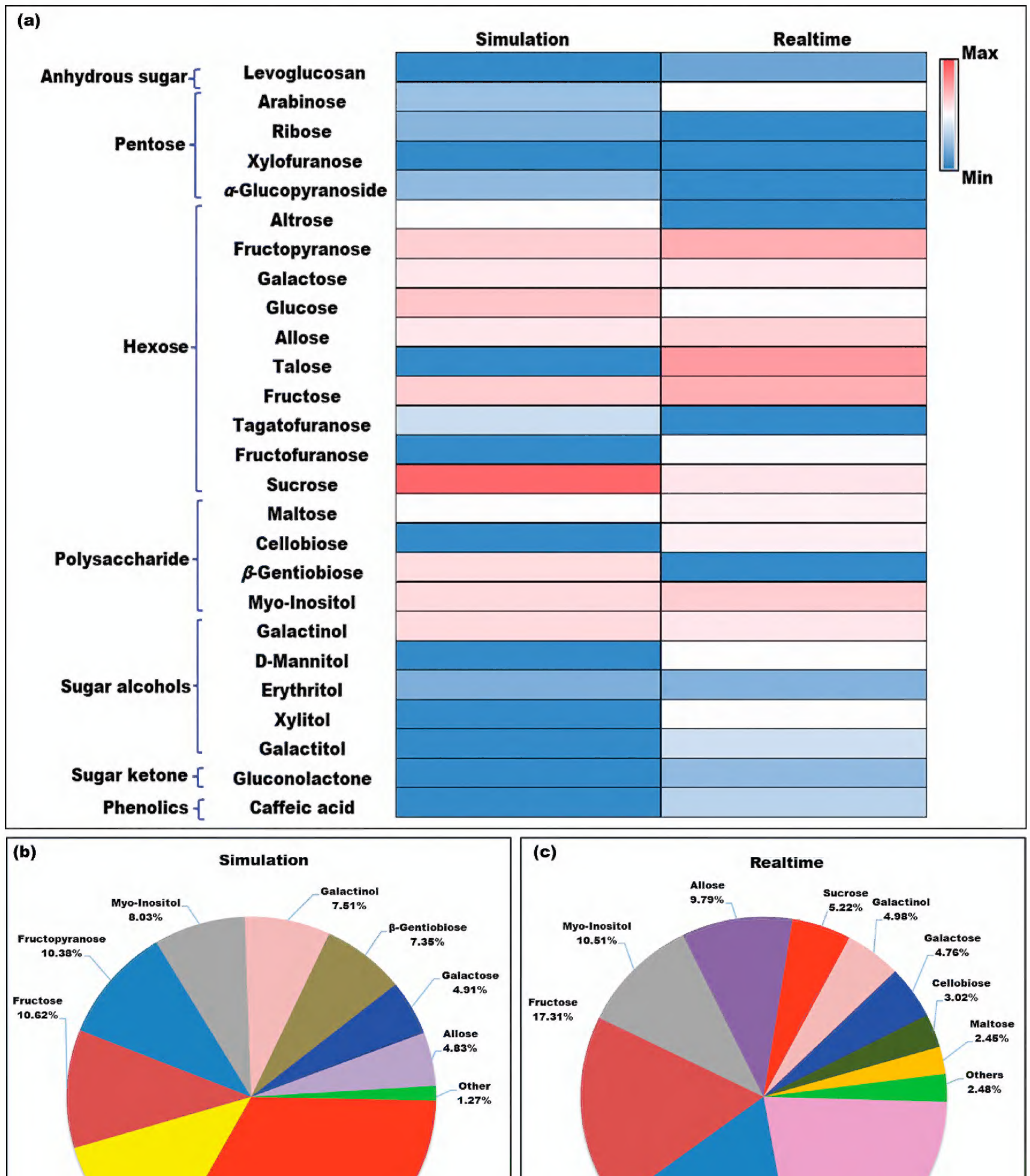

Figure 2. Heatmap showing a comparison between relative abundance of different primary metabolites (grouped under various categories) found in the red leaves from simulation experiment and realtime experiment (**a**). Pie chart showing major components of primary metabolites for simulation experiment (**b**) and for realtime experiment (**c**).

Discussion

The key finding of this experiment was the successful postharvest anthocyanin accumulation in detached leaves when kept in open environment. Simulation experiment also suggested that the detached leaves can withstand temperature fluctuations as occurred at realtime situation in open temperate environment. The differences in the patterns of anthocyanin and rosmarinic acid accumulation in detached leaves incubated at two defined conditions raised many questions about any possible changes occurred in the levels of accumulated primary metabolites that might have channelized towards specialized metabolism. The main question is whether these differences in accumulation pattern are solely due to variation in different

sugar levels or not. Changes in the sugar concentrations were clearly visible between the simulation and realtime experiments. These significant changes in different sugar concentrations provide a clue for modulation of rosmarinic acid and the mechanism behind the anthocyanin accumulation in detached leaves.

One important thing that needs to be considered here is the status of the leaves; these postharvest detached leaves served as a store for reserved starch granules which were the only source of available carbon pool to synthesize anthocyanin rather than other photosynthates (Wang et al. 2016). This was confirmed by the presence of maltose (a starch breakdown product) in detached leaves from both simulation and realtime experiments. Starch broken down to sucrose which subsequently produced a massive amount of glucose-6-phosphate that driven the anthocyanin biosynthesis in postharvest leaves via the shikimate-phenylpropanoid pathway (Wang et al. 2016). This hypothesis can be supported from the metabolite profiling data, where the presence of erythritol was confirmed (Fig. 3). This sugar alcohol is produced from erythrose-4-phosphate as an intermediate of pentose phosphate pathway (Nakagawa et al. 2020).

Further, rosmarinic acid content was also found to be higher in the detached leaves from realtime experiment in comparison to simulation experiment. However, higher cyanidin content was reported from simulation experiment as compared to realtime experiment. This could be due to the formation of more sucrose from breakdown of starch as detected in simulation experiment resulting eventually in more glucose, glyceraldehyde-3-phosphate and malonyl-CoA formation leading to more cyanidin accumulation rather than rosmarinic acid (De Vega et al. 2021) (Fig. 3). This proposition can be supported from the data of sucrose and glucose percentage; which were highest in the profile of primary metabolites from the detached leaves of simulation experiment. This can be further strengthened by the presence of β-gentiobiose only in the profile of primary metabolites from detached leaves of simulation experiment. Formation of β-gentiobiose basically occurred from the acid-catalyzed condensation reaction of two D-glucose molecules joined with a β-1,6 linkage (Zhang et al. 2023). We assumed that accumulation of glucose in a very high concentration perhaps led to its non-enzymatic conversion into β-gentiobiose, a rare sugar usually found in a perennial herb *Gentiana* sp. (Takahashi et al. 2014).

In case of realtime experiment, a lower amount of sucrose was detected, which led to a reduced amount of malonyl-CoA formation. Therefore, most of the *p*-coumaroyl-CoA was possibly utilized in rosmarinic acid biosynthesis rather than reacting with malonyl-CoA to channelize towards the formation of naringenin chalcone, an early precursor of anthocyanin biosynthesis (Yamazaki et al. 2003) (Fig. 3). This hypothesis is further supported from the observation of caffeic acid accumulation only in realtime experiment. Caffeic acid is usually formed from *p*-coumaroyl-CoA via successive formation of *p*-coumaroyl-shikimate and caffeoyl shikimate (Lin et al. 2015; Deguchi and Ito 2020; Kwon et al. 2021). Therefore, utilization

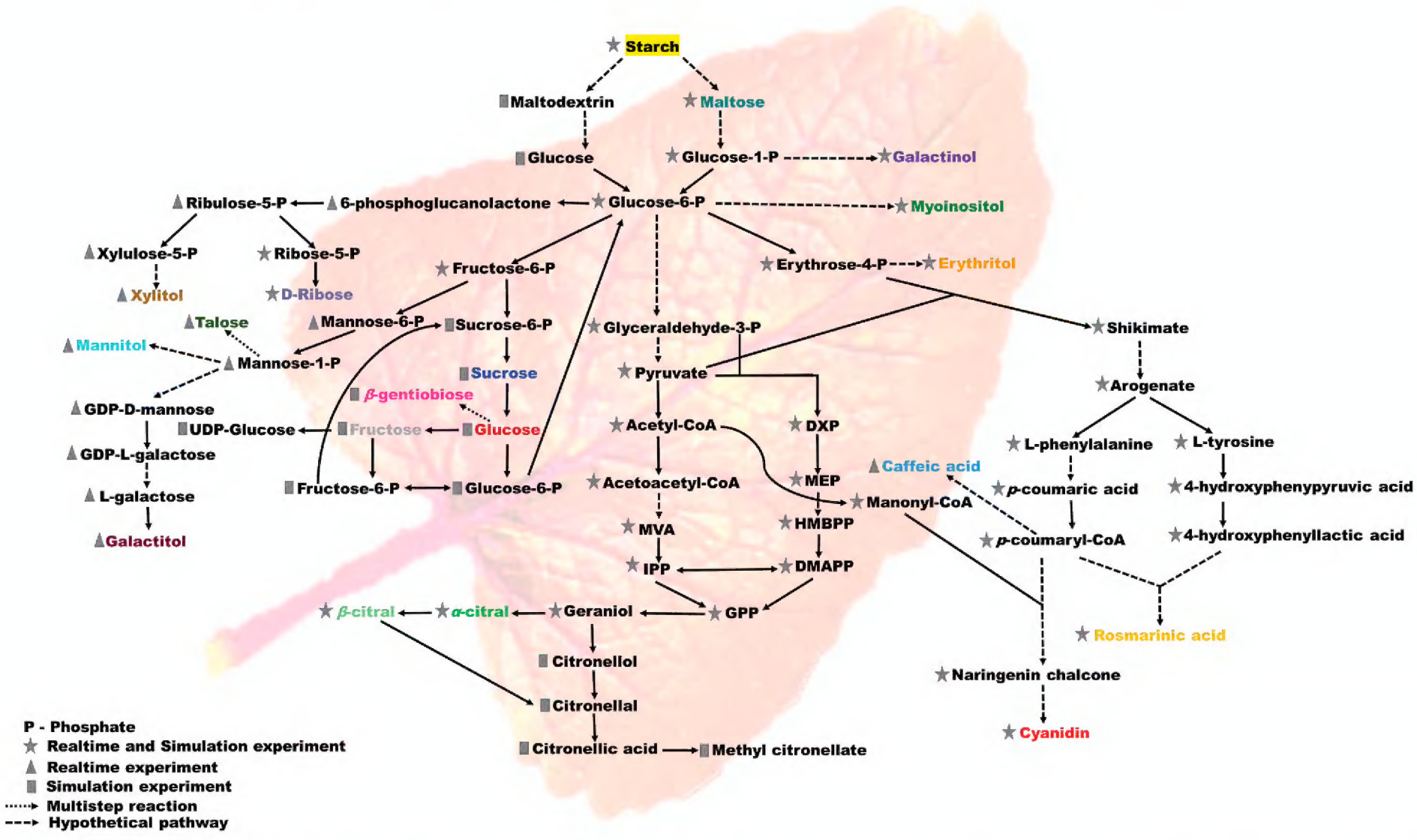

Figure 3. Hypothetical pathway mapped based on all the major biochemical pathways contributing to the accumulation of primary metabolites found in postharvest detached leaves. The metabolite profiling data generated from simulation and realtime experiments formed the backbone of this hypothesis. Major metabolites are marked in different colour.

of *p*-coumaroyl-CoA towards the formation of caffeic acid esters including rosmarinic acid limits its availability to react with malonyl-CoA for ultimate formation of anthocyanins.

In case of realtime experiment, the percentage of talose was found to be very high among the primary metabolites which could be due to the formation of more mannose and xylulose rather than sucrose from glucose-6-phosphate arose as a breakdown product of starch (Williamson et al. 2002; Orzechowski et al. 2008). As a result, formation of mannitol, galactitol and xylitol was found in realtime experiment, which are basically the sugar alcohol derivatives of the mannose, galactose and xylulose, respectively. Interestingly, talose is also a C-2 epimer of galactose and a C-4 epimer of mannose (Fig. 3). As most of the pyruvates (generated from the breakdown of starch) and acetyl-CoA were channelized towards shikimate/phenylpropanoid pathway for the formation of either rosmarinic acid or cyanidin, as a consequence, utilization of reserved carbon pools to form terpenoid volatiles such as, citral via MVA and/or MEP pathways was possibly hindered (Delle-Vedove 2011; Da Silva Souza et al. 2020; Yeon and Kim 2020). Such limit of precursor availability for MVA and MEP pathways led to degradation of volatiles internal pool (Fig. 3). Further, cellobiose was also found along with the other sugars present in the detached leaves from realtime experiment. Cellobiose is actually degradation product of a key cell wall component cellulose (Aro et al. 2005; Van De Wouwer et al. 2018). However, the reason for cellobiose accumulation remained unclear.

Further, attempts were also made to make various value-added food products from these red leaves. First of all, dried leaves itself can be directly used as garnishing agent for any food preparations. Besides, we used lemon juice to extract the anthocyanin from leaves without use of any mineral acid or even synthetic organic acid for any food-grade use in several other preparations accordingly e.g., in garnishing of fruit salads. We have shown here three such food preparations made from the extracted juice of red lemon balm leaves namely, cake, herbal tea and ice cubes (Fig. 4). All of these were tested by many unbiased

Figure 4. Various food products prepared from the value-added leaves of lemon balm. Fine powder made from dried leaves (200 mg) was extracted with fresh lemon juice (pH 1) to release anthocyanins in aqueous phase. The anthocyanin rich colour juice was mixed with icing sugar followed by spreading over the cake and finally kept in refrigerator for overnight. Herbal tea was prepared from dried leaves dipped in hot water containing few drops of lemon juice.

individuals who provided positive feedback without any irritation or side-effects after intake.

Conclusions

Detached leaves of lemon balm accumulating anthocyanin under simulated condition of changing air temperature as well as in realtime experiment now provided a strong base for carrying out the experiment in open environment. Several interesting perturbations were also observed in the marker phenolics, volatile compounds and also in the profile of non-volatile metabolites - all of these were able to provide key clues on the possible the mechanism behind this unusual anthocyanin accumulation in postharvest leaves as discussed earlier. However, to strengthened the hypothesis, enzyme activities and gene expression analyses need to be carried out in near future. Various food products were also prepared from these value-added leaves to demonstrate its applicability in both home scale and community-based initiatives to uplift livelihood.

Conflicts of interest

No potential conflict of interest was reported by the authors.

Contribution of authors

Pritam Kumar Dey - Investigation, methodology and draft manuscript preparation. Manisha Lakhanpal - Investigation. Adinpunya Mitra - Conceptualization, obtained funding and manuscript editing.

Acknowledgements

This work was supported by the Department of Science & Technology, Government of India [DST/SEED/ASACO-DER-135-061/2018 to A Mitra]. A senior research fellowship was awarded to P K Dey from this grant. Mrs. Dalia Mitra is acknowledged for her contribution during the food products preparation.

References

Aro N, Pakula T, Penttilä M (2005) Transcriptional regulation of plant cell wall degradation by filamentous fungi. FEMS Microbiology Review 29: 719–739. https://doi.org/10.1016/j.femsre.2004.11.006

Barman M, Mitra A (2019) Temporal relationship between emitted and endogenous floral scent volatiles in summer-and winter-blooming *Jasminum* species. Physiologia Plantarum 166: 946–959. https://doi.org/10.1111/ppl.12849

Burt S (2004) Essential oils: their antibacterial properties and potential applications in foods - a review. International Journal of Food Microbiology 94: 223–253. https://doi.org/10.1016/j.ijfoodmicro.2004.03.022

Cisse M, Vaillant F, Kane A, Ndiaye O, Dornier M (2012) Impact of the extraction procedure on the kinetics of anthocyanin and colour degradation of roselle extracts during storage. Journal of the Science of Food and Agriculture 92: 1214–1221. https://doi.org/10.1002/jsfa.4685

da Silva Souza MA, Peres LE, Freschi JR, Purgatto E, Lajolo FM, Hassimotto NM (2020) Changes in flavonoid and carotenoid profiles alter volatile organic compounds in purple and orange cherry tomatoes obtained by allele introgression. Journal of the Science of Food and Agriculture 100: 1662–1670. https://doi.org/10.1002/jsfa.10180

Deguchi Y, Ito M (2020) Caffeic acid and rosmarinic acid contents in genus *Perilla*. Journal of Natural Medicines 74: 834–839. https://doi.org/10.1007/s11418-020-01418-5

Delle-Vedove R, Juillet N, Bessière JM, Grison C, Barthes N, Pailler T, Dormont L, Schatz B (2011) Colour-scent associations in a tropical orchid: Three colours but two odours. Phytochemistry 72: 735–742. https://doi.org/10.1016/j.phytochem.2011.02.005

De Vega JJ, Peel N, Purdy SJ, Hawkins S, Donnison L, Dyer S, Farrar K (2021) Differential expression of starch and sucrose metabolic genes linked to varying biomass yield in *Miscanthus* hybrids. Biotechnology for Biofuels 14: 1–15. https://doi.org/10.1186/s13068-021-01948-4

Dey PK, Goswami A, Mitra A (2023) A new targeted approach of postharvest accumulation of anthocyanin in fragrant leaves of *Melissa officinalis* L. Industrial Crops and Products 196: 116479. https://doi.org/10.1016/j.indcrop.2023.116479

Kotamreddy JNR, Hansda C, Mitra A (2020) Semi-targeted metabolomic analysis provides the basis for enhanced antioxidant capacities in pigmented rice grains. Journal of Food Measurement and Characterization 14: 1183–1191. https://doi.org/10.1007/s11694-019-00367-2

Kwon DY, Kim YB, Kim JK, Park SU (2021) Production of rosmarinic acid and correlated gene expression in hairy root cultures of green and purple basil (*Ocimum basilicum* L.). Preparative Biochemistry & Biotechnology 51: 35–43. https://doi.org/10.1080/10826068.2020.1789990

Lin CY, Wang JP, Li Q, Chen HC, Liu J, Loziuk P, Song J, Williams C, Muddiman DC, Sederoff RR, Chiang VL (2015) 4-Coumaroyl and caffeoyl shikimic acids inhibit 4-coumaric acid: coenzyme A ligases and modulate metabolic flux for 3-hydroxylation in monolignol biosynthesis of *Populus trichocarpa*. Molecular Plant 8: 176–187. https://doi.org/10.1016/j.molp.2014.12.003

Meftahizade H, Lotfi M, Moradkhani H (2010) Optimization of micropropagation and establishment of cell suspension culture in *Melissa officinalis* L. African Journal of Biotechnology 9: 4314–4321.

Nakagawa Y, Kasumi T, Ogihara J, Tamura M, Arai T, Tomishige K (2020) Erythritol: Another C4 platform chemical in biomass refinery. ACS Omega 5: 2520–2530. https://doi.org/10.1021/acsomega.9b04046

Nyman NA, Kumpulainen JT (2001) Determination of anthocyanidins in berries and red wine by high-performance liquid chromatography. Journal of Agricultural and Food Chemistry 49: 4183–4187. https://doi.org/10.1021/jf010572i

Orzechowski S (2008) Starch metabolism in leaves. Acta Biochimica Polonica 55: 435–445. https://doi.org/10.18388/abp.2008_3049

Pistelli L, Tonelli M, Pellegrini E, Cotrozzi L, Pucciariello C, Trivellini A, Nali C (2019) Accumulation of rosmarinic acid and behaviour of ROS processing systems in *Melissa officinalis* L. under heat stress. Industrial Crops and Products 138: 111469. https://doi.org/10.1016/j.indcrop.2019.111469

Qin C, Li Y, Niu W, Ding Y, Zhang R, Shang X (2010) Analysis and characterisation of anthocyanins in mulberry fruit. Czech Journal of Food Sciences 28: 117–126. https://doi.org/10.17221/228/2008-CJFS

Rao KS, Haran RH, Rajpoot VS (2022) Value addition: A novel strategy for quality enhancement of medicinal and aromatic plants. Journal of Applied Research on Medicinal and Aromatic Plants 31: 100415. https://doi.org/10.1016/j.jarmap.2022.100415

Taban BM, Stavropoulou E, Winkelströter LK, Bezirtzoglou E (2021) Value-added effects of using aromatic plants in foods and human therapy. Journal of Food Science and Technology 42. https://doi.org/10.1590/fst.43121

Takahashi H, Imamura T, Konno N, Takeda T, Fujita K, Konishi T, Nishihara M, Uchimiya H (2014) The gentio-oligosaccharide gentiobiose functions in the modulation of bud dormancy in the herbaceous perennial *Gentiana*. Plant Cell 26: 3949–3963. https://doi.org/10.1105/tpc.114.131631

Van de Wouwer D, Boerjan W, Vanholme B (2018) Plant cell wall sugars: sweeteners for a bio-based economy. Physiologia Plantarum 164: 27–44. https://doi.org/10.1111/ppl.12705

Wang S, Pan D, Lv X, Song X, Qiu Z, Huang C, Huang R, Chen W (2016) Proteomic approach reveals that starch degradation contributes to anthocyanin accumulation in tuberous root of purple sweet potato. Journal of Proteomics 143: 298–305. https://doi.org/10.1016/j.jprot.2016.03.010

Williamson JD, Jennings DB, Guo WW, Pharr DM, Ehrenshaft M (2002) Sugar alcohols, salt stress, and fungal resistance: polyols—multifunctional plant protection? Journal of the American Society for Horticultural Science 127: 467–473. https://doi.org/10.21273/JASHS.127.4.467

Yamazaki M, Nakajima JI, Yamanashi M, Sugiyama M, Makita Y, Springob K, Awazuhara M, Saito K (2003) Metabolomics and differential gene expression in anthocyanin chemo-varietal forms of *Perilla frutescens*. Phytochemistry 62: 987–995. https://doi.org/10.1016/S0031-9422(02)00721-5

Yeon JY, Kim WS (2020) Floral pigment-scent associations in eight cut rose cultivars with various petal colors. Horticulture, Environment, and Biotechnology 61: 633–641. https://doi.org/10.1007/s13580-020-00249-3

Zhang S, Ni D, Zhu Y, Xu W, Zhang W, Mu W (2023) A comprehensive review on the properties, production, and applications of functional glucobioses. Critical Reviews in Food Science and Nutrition: 1–14. https://doi.org/10.1080/10408398.2023.2261053